Multielectron processes in 10-keV/u Ar^{q+} ($5 \leq q \leq 17$) on Ar collisions

R. Ali, C. L. Cocke, M. L. A. Raphaelian, and M. Stockli
J. R. Macdonald Laboratory, Department of Physics, Kansas State University, Manhattan, Kansas 66506-2604
(Received 24 June 1993)

We have used time-of-flight coincidence techniques to study multielectron reactions in 10-keV/u ($v=0.632$ a.u.) Ar^{q+} ($5 \leq q \leq 17$) on Ar collisions. Absolute cross sections for total charge-transfer (σ_q), projectile charge-change ($\sigma_{q,q-k}$), recoil production (σ_q^i), and phenomenological cross sections ($\sigma_{q,q-k}^i$) have been obtained by normalizing to cross sections reported in the literature [H. Klinger, A. Müller, and E. Salzborn, J. Phys. B **8**, 230 (1975)]. The data have been used to critically test the predictions of the molecular classical overbarrier model (MCBM) [A. Niehaus, J. Phys. B **19**, 2925 (1986)] and rather impressive agreements have been obtained. In particular, the predictions of target outer-shell excitation seem to have supporting evidence in this set of data. A stabilization scheme for the multiply excited projectile following charge transfer is proposed to complement the MCBM predictions and the gross features of the final reaction products are fairly accounted for. In addition, enhanced electron loss from the projectile-target system is observed in hard collisions for low-charged projectiles ($q \leq 8$) and is attributed to inner-shell excitation via molecular-orbital promotion.

PACS number(s): 34.70.+e, 34.50.Fa

I. INTRODUCTION

Collisions of slow multiply charged ions with multielectron target atoms (molecules) have been extensively investigated for nearly two decades by now. It is established that the dominant target electron removal mechanism in such collisions is electron capture. Substantial progress has been made in understanding collision systems with two active electrons, both theoretically in terms of the quasimolecular description of the collision process and experimentally through total and differential cross-section measurements and by utilizing energy-gain, Auger electron, and photon spectroscopic techniques. For a recent review on the progress made in this field we refer the reader to the review by Barat and Roncin [1].

On the other hand, systems with more than two active electrons have received less attention and still pose tremendous challenges. Experimentally, it is difficult to disentangle the phenomenological final reaction products to deduce information on the collision process itself and quantum-mechanical theoretical treatment is out of reach due to the large number of involved channels. Following the early projectile charge-change cross-section measurements by Klinger, Müller, and Salzborn [2] and the application of coincidence techniques by Cocke *et al.* [3], a number of experimental cross sections differential in both recoil and final projectile charge states have been made available [4–8]. In addition, recoil charge-state fractions in coincidence with final projectile charge states [9] and in single mode [10] have been reported. A few energy-gain measurements involving more than double-electron capture have been carried out [11–15] and a similar situation holds for investigations of angular dependence and differential cross sections [8,16–19]. The employment of Auger electron spectroscopy to study such collisions [20–22] is still in its infancy and in this respect the pioneering work by Posthumus and Morgenstern [21] is acknowledged. In addition, photon emission from Rydberg transitions in collisions of highly charged ions with multielectron targets has been investigated by Martin *et al.* [23–26].

The accumulation of experimental results awaiting proper interpretation has led to the extension of the classical overbarrier model [27] to include multiple-capture processes in the form of the extended classical overbarrier model by Bárány *et al.* [28], which was followed by the more sophisticated molecular classical overbarrier model (MCBM) by Niehaus [29]. Confronted with experimental results, both models have reasonably accounted for recoil production cross sections, energy-gain spectra, differential cross sections, and some phenomenological cross sections. Of the two, the MCBM has more predictive powers and has ben subjected to several critical tests. For example, target excitation is one of several processes the model predicts. However, it has been criticized for overestimating this process [8,19] and it is generally believed that the transfer of i electrons to the projectile is best signaled by the detection of a recoil with charge state i, while the final charge state of the projectile is determined by the different stabilization channels of the multiply excited projectile as described by

$$A^{q+}+B \rightarrow A^{(q-i)+*}+B^{i+} \tag{1a}$$

$$\rightarrow A^{(q-k)+}+B^{i+}+(i-k)e^{-}+\gamma\ . \tag{1b}$$

Cederquist *et al* [30] reported on target excitation in collisions of very highly charged ions with two-electron targets but not for multielectron targets in the case of two-electron processes. Nevertheless, photon emission from multielectron targets, an indication of target excitation, has been detected by Martin *et al.* [22,23].

Furthermore, while the model has been acknowledged for reasonably accounting for the transfer of electrons to the projectile, it has been argued that a shortcoming of

the model is its inability to account for the final projectile charge state [1]. It is essential, at this point to stress that the aforementioned criticism was based on experiments which in most cases involved moderately charged projectiles ($q \leq 10$), and in many cases not all the final projectile charge states have been registered, which makes the comparison with the model predictions subject to the assumptions of the individual investigators. Indeed, the model in its present form stops at giving the final capture state distribution on the projectile and therefore its inability to provide the final projectile charge state does not necessarily constitute a shortcoming. Instead, this capture state distribution should be a starting point for developing a stabilization scheme for the multiply excited projectile.

In this work, we report the experimental measurements of total charge-transfer (σ_q), recoil production (σ_q^i), projectile charge-change ($\sigma_{q,q-k}$), and phenomenological cross sections ($\sigma^i_{q,q-k}$, where $\sigma^i_{q,q'}$ is the cross section for initial projectile charge state q producing a recoil in charge state i and finally being detected in charge state q') for Ar^{q+} ($5 \leq q \leq 17$) on Ar collision systems at a fixed collision energy of 400 keV ($v = 0.632$ a.u.). Recoil charge states up to $i = 8$ have been observed and up to a quintuple projectile charge change has been identified. The data are presented in various forms to allow for proper comparison with the MCBM predictions. A stabilization scheme for the multiply excited projectiles which utilizes the capture state distribution given by the MCBM is proposed in an attempt to account for the various phenomenological aspects of the final reaction products. In addition, evidence for inner-shell excitation via molecular-orbital promotion has been observed and will be discussed.

II. EXPERIMENT

The experimental setup is shown in Fig. 1. The 10-keV/u Ar^{q+} ion beams were provided by the Kansas State University Cryogenic Electron-Beam Ion Source [31]. The beams were collimated and limited in size to 0.3 mm by a four-jaw slit and the collision chamber entrance aperture which were separated by about 3.5 m. The Ar gas target was furnished by a multichannel array molecular jet [32], and the gas flow was adjusted to minimize double collisions, with an estimated effective target density of 0.2–0.5 mTorr depending on the incident projectile charge state. After the collision, the recoil ions

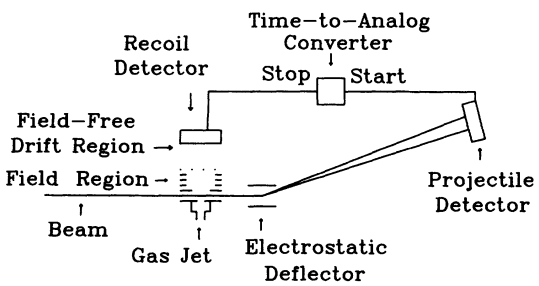

FIG. 1. Schematic of the experimental setup.

were extracted transverse to the beam direction by a uniform electric field (≈ 10 V/cm). The field was maintained by an acceleration column consisting of ten thin (0.13 mm) gold-plated square brass plates (50 mm × 50 mm) with center holes of 38 mm diameter. After exiting the field region (2 cm) the recoil ions traveled 4 cm in a field-free drift region before being detected by a channel-plate detector. A parallel-plate electrostatic deflector separated the final projectile charge states which were then detected by a two-dimensional position-sensitive channel-plate detector located 1.2 m downstream from the collision chamber. A coincident time-of-flight technique was used to determine the recoil charge states. The collision chamber was differentially pumped such that high ion beam purities were maintained prior to entering the chamber and after exiting it and entering the electrostatic analysis region. Typical pressures of about 4×10^{-9} and 3×10^{-7} Torr were maintained upstream and downstream, respectively, while the residual gas pressure in the chamber was about 6×10^{-7} Torr.

The data were collected in two modes. The first comprised detecting only those projectiles that changed their charge states by deflecting the main beam (2–10 kHz) away from the detector. This allowed for the registration of coincidence events (50–250 Hz) corresponding to charge transfer where three different final projectile charge states could be detected each run. For $q \geq 10$, no more than triple projectile charge change ($k = 5$) was observed and therefore additional runs were needed. In these cases, the triple charge-change channel was always in common to allow for proper normalization. An example of the raw data collected in this mode is shown as a density plot in Fig. 2 for the case of Ar^{13+}. Such a plot allows for an unambiguous high recoil charge-state separation, taking advantage of the collision kinematics as manifested by the tilts in the density distributions. These tilts are due to the fact that recoil ions that are initially scattered toward the recoil detector (corresponding to projectiles scattered toward large-x positions) take less time to reach the detector than the ones scattered away from the detector (corresponding to projectiles scattered toward small-x positions). One observes the presence of double-collision events signaled by the detection of recoil charge state $i = 1$ (2) in coincidence with double (triple) projectile charge change. These events were used in an iterative correction process such that the data finally represented single-collision processes.

The second mode of data acquisition aimed at obtaining absolute cross sections for the previously measured coincidence events. This was done by detecting the main beam (0.5–1 kHz) together with the projectile charge-change channels in singles and coincidence modes simultaneously for all projectile charge states at 10 keV/u and at a fixed gas target flow. The coincidence data allowed for double-collision corrections. Capture on the residual gas was also registered with no gas flow and final single projectile charge-change probabilities were obtained and were all normalized to that of Ar^{7+}.

In a similar fashion, the single projectile charge-change probability for Ar^{7+} at 10 keV/u (400 keV) was normalized to that of Ar^{7+} at 70 keV for which an absolute

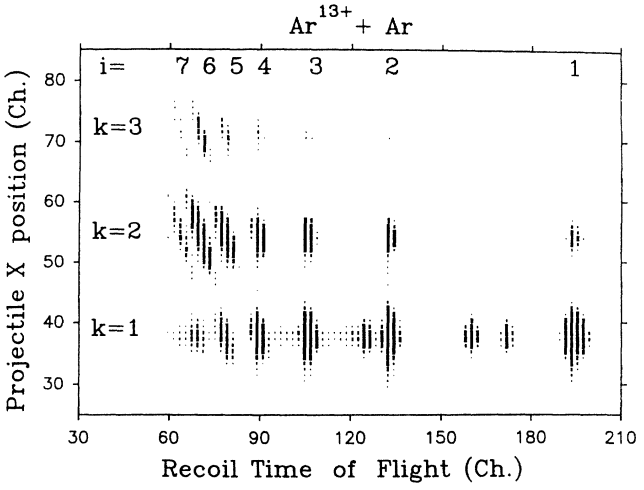

FIG. 2. A density plot of the projectile x position vs recoil time of flight for the (Ar^{13+}+Ar) collision system. Recoil charge states are indicated by i and the degrees of projectile charge-change are indicated by k.

cross section was measured by Klinger, Müller, and Salzborn [2]. Having obtained $\sigma_{7,6}$ at 10 keV/u, all other projectile charge-change cross sections as well as total charge-transfer cross sections were also obtained and are shown in Fig. 3. We notice that σ_q and $\sigma_{q,q-1}$ exhibit nearly linear dependence on q, while $\sigma_{q,q-2}$ and $\sigma_{q,q-3}$ seem to complement each other. Together with the coincidence measurements, the projectile charge-change cross

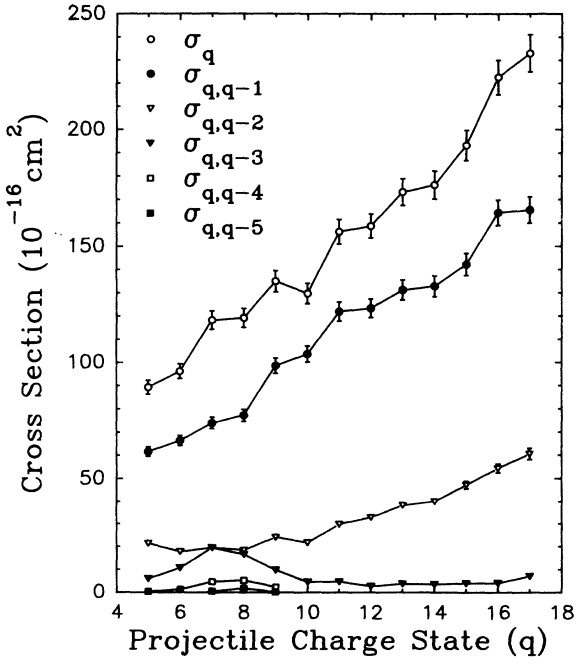

FIG. 3. Projectile charge-change cross sections ($\sigma_{q,q-k}$) and total charge-transfer cross section ($\sigma_q=\sum_k \sigma_{q,q-k}$) for 10-keV/u Ar^{q+} on Ar. The error bars comprise statistical, double-collision correction, and reproducibility uncertainties. A maximum additional error of 30% in the measured $\sigma_{7,6}$ [1] to which these data were normalized should be incorporated.

sections provide phenomenological and recoil production cross sections which will be presented in Sec. IV.

III. THE MOLECULAR CLASSICAL OVERBARRIER MODEL

Most of the discussion will be based on the molecular classical overbarrier model and therefore a somewhat detailed description of its main features is given. The model distinguishes between two parts in the collision process, the way in and the way out. On the way in and as the incident ion A^{q+} approaches the target atom B, the Coulomb potential barrier separating the target electrons from regions around A decreases in height with decreasing internuclear separation R until a turning point is reached. As the barrier decreases, it ceases to be effective for the target electrons in order of increasing ionization potentials I_t at internuclear separations R_t^i determined by matching the barrier height with the Stark-shifted binding energy for the tth electron. Each electron for which the barrier is no longer effective is assumed to become molecular in such a way that it does not shield the incident ion or the residual target ion, and it is still characterized by its initial Stark-shifted binding energy.

On the way out, the Coulomb barrier starts increasing with increasing R and becomes effective for the molecular electrons in order of decreasing binding energies at distances R_t^o, which are also determined by matching the barrier height with the original Stark-shifted binding energy of the ith electron, which is assumed to have remained the same during the collision. At R_t^o, the concerned electron has finite probabilities to be captured by the projectile onto a state with principal quantum number n_t or recaptured by the target onto a state with quantum number m_t. The ratio of these probabilities is taken to be the ratio of degeneracies of the state n_t or m_t on A or B. In the hydrogenic approximation, the probability for capture is thus given by

$$W_t=n_t^2/(n_t^2+m_t^2) \tag{2}$$

and, for recapture by the target, by $1-W_t$. Once an inner electron is captured or recaptured it is assumed to fully screen the corresponding ionic core as far as the remaining molecular electrons are concerned. In this perspective a single collision event may be described by a string (j) whose elements are either 1 or 0 indicating capture by A or recapture by B and where the positions of the elements indicate the indices of the electrons in order of increasing binding energies. For example, the string (j)=(01010100) implies that eight electrons were molecularized during the collision, out of which the electrons characterized by the second, fourth, and sixth target ionization energies were captured by the projectile while the remaining electrons were recaptured by the target. The asymptotic binding energies of the tth electron on A or B are obtained by matching the original Stark-shifted binding energy evaluated at R_t^i with the Stark-shifted binding energies on A or B evaluated at R_t^o and are given by

$$EA_t(r_t)=I_t+\frac{q}{R_t^i}-\frac{t+r_t}{R_t^o(r_t)}\ , \tag{3a}$$

$$EB_t(r_t)=I_t+\frac{q}{R_t^i}-\frac{q-r_t}{R_t^o(r_t)} , \tag{3b}$$

where r_t is the number of electrons with indices greater than t and that have been captured by A. Niehaus [29] pointed out that the quantum numbers n_t and m_t could be obtained with various degrees of sophistication depending on the collision system. For our collision systems they are evaluated from the asymptotic binding energies with the proper introduction of the quantum defects

$$n_t(r_t)+d_q(r_t)=\frac{q-r_t}{[2EA_t(r_t)]^{1/2}} , \tag{4a}$$

$$m_t(r_t)+d_t(r_t)=\frac{t+r_t}{[2EB_t(r_t)]^{1/2}} , \tag{4b}$$

where d_q and d_t are the projectile and target quantum defects, respectively, and are given by

$$d_q(r_t)=\frac{q+1}{[2I_{q+1}]^{1/2}}-n_0 , \tag{5a}$$

$$d_t(r_t)=\frac{t+r_t}{[2I_{t+r_t}]^{1/2}}-m_0 , \tag{5b}$$

where n_0 and m_0 are the quantum numbers of the outer shells of A^{q+} and B, and I_{q+1} and I_{t+r_t} are the $(q+1)$th and $(t+r_t)$th ionization potentials of A^{q+} and B, respectively. In Eq. (5b) the target quantum defect varies with the degree of target ionization and it ensures recapture into the original shell if $r_t=0$, while in Eq. (5a) the projectile quantum defect is taken to be fixed. Fixing the projectile quantum defect is not an unreasonable assumption for projectiles with $q \leq 8$, for which the electrons are captured to partially filled or low lyings n's and it has much less effect for $q \geq 9$. Furthermore, fixing the quantum defect partially compensates for the assumption that the captured electrons fully screen the ionic core as viewed by the remaining molecular electrons.

Absolute cross sections are then assigned to each string through products of probabilities and geometrical cross sections $A_t=\pi[(R_t^i)^2-(R_{t+1}^i)^2]$ for $t<t_{\max}$ and $A_{t_{\max}}=\pi(R_{t_{\max}}^i)^2$, where $t_{\max}$ is the index of the most bound electron that became molecular. In this model, the number of electrons that may become molecular is equal to the minimum of either the projectile charge state or the number of electrons N in the target outermost shell. Therefore, there would be $\binom{N}{r}$ or $\binom{q}{r}$ strings contributing to the transfer of r electrons to the projectile. Generally, the model predicts capture to populate excited levels of the projectile, and if two or more inner target electrons are captured, outer electrons are recaptured and the target is left in a multiply excited state.

IV. RESULTS AND DISCUSSION

A. Total charge-transfer and recoil production cross sections

The simplest prediction of the MCBM concerns the total charge-transfer cross section σ_q. Only two quantities are needed to evaluate this cross section, the geometrical cross section $[\sigma_{\text{geom}}=\pi(R_1^i)^2]$, corresponding to molecularizing the least bound electron, and the cross section for no charge transfer $(\sigma_{q,q}^0)$ which is described by the string $(j)=(00\cdots0)$. The difference between these two cross sections is the total charge-transfer cross section

$$\sigma_q=\sigma_{\text{geom}}-\sigma_{q,q}^0 . \tag{6}$$

In Fig. 4 we show the experimental σ_q and the model σ_q, σ_{geom}, and $\sigma_{q,q}^0$. At a glance, very good agreement between the model prediction and the experiment is observed. It might appear that σ_{geom} is in better agreement with the experiment; however, this cannot be substantiated within the error bars (with an additional 30% from the normalization process). One cannot exclude the possibility that the observed overall remarkable agreement of absolute cross sections between the experiment and the MCBM predictions is fortuitous and specific to this collision velocity. Although it is widely believed that charge exchange cross sections are weakly dependent on the collision velocity for $v<1$ a.u., such a belief is based on measurements the majority of which involved $v<0.5$ a.u. Extending the measurements to higher velocities is therefore essential in order to remove any doubts.

Experimental recoil production cross sections are obtained by summing the phenomenological cross sections, obtained from the coincidence measurements, over all final projectile charge states $(\sigma_q^i=\sum_k \sigma_{q,q-k}^i)$. These cross sections are compared with the MCBM predictions in two ways. First, the recoil charge state (i) is assumed to be equal to the number of electrons (r) transferred to the projectile, which corresponds to fully suppressing any

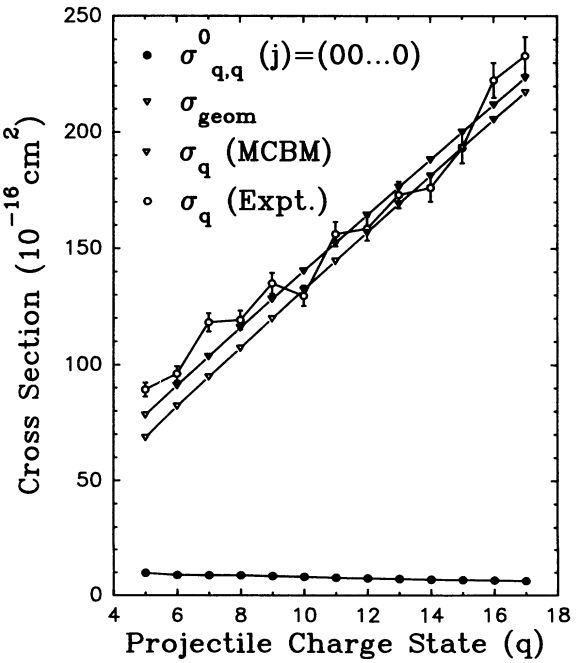

FIG. 4. Experimental total transfer cross sections and MCBM geometrical, no charge-transfer, and total charge-transfer cross sections.

possible target autoionization. The MCBM σ_q^i is then obtained by summing the cross sections of all strings (j) representing the transfer of i electrons. The resulting cross sections are shown in Fig. 5 for all observed recoil charge states. An overall reasonable agreement is observed. However, a general tendency for underestimating the cross sections for recoil charge states $i > 4$ is obvious for the lower projectile charge states ($q < 9$) and for all projectile charge states in the case of $i \geq 6$. The next logical comparison should involve the predicted target autoionization. This requires the inspection of each individual string representing the transfer of r electrons to the projectile for possible target autoionization. In this fashion, the recoil charge state is determined by the transfer of r electrons in addition to the loss of one or two electrons via autoionization. We have assumed target autoionization to proceed whenever energetically allowed in the sense that multiply excited states of the target that are forbidden to autoionize by selection rules are assumed to be statistically negligible. The results so obtained are compared to the experiment in Fig. 6. Clearly, allowing for target autoionization results in much better agreement for the high recoil charge states (except $i = 8$) and for all projectile charge states. The lack of structures in the MCBM cross sections results from the assumption that the quantum numbers n_t and m_t are continuous. We notice that there is no difference at all between Figs. 5 and 6 for $i = 1$ and only very little difference for $i = 2$. The latter is consistent with the observation by Cederquist *et al.* [30] that two-electron transfer-excitation processes are less important for multielectron targets than for two-electron targets. The situation is substantially different for $i \geq 3$ for which target excitation seems to play an important role as deduced from our measurements and the MCBM predictions, and therefore the collision process may be best described by

$$A^{q+} + B \rightarrow A^{(q-r)+*} + B^{r+*} \tag{7a}$$

$$\rightarrow A^{(q-k)+} + B^{i+} + (i-k)e^- + \gamma \ . \tag{7b}$$

Our inference of the importance of target outer-shell excitation in hard collisions leading to the production of multiply charged recoil ions has been based on comparisons with the MCBM predictions and does not constitute a direct proof that it actually happens. Settling this issue would require direct observation of target autoionization. While identifying target Auger lines might be a formidable task in singles Auger spectra due to the dominance of projectile Auger lines, proper choice of both projectile and target species to minimize the overlap of the expected Auger lines together with the employment

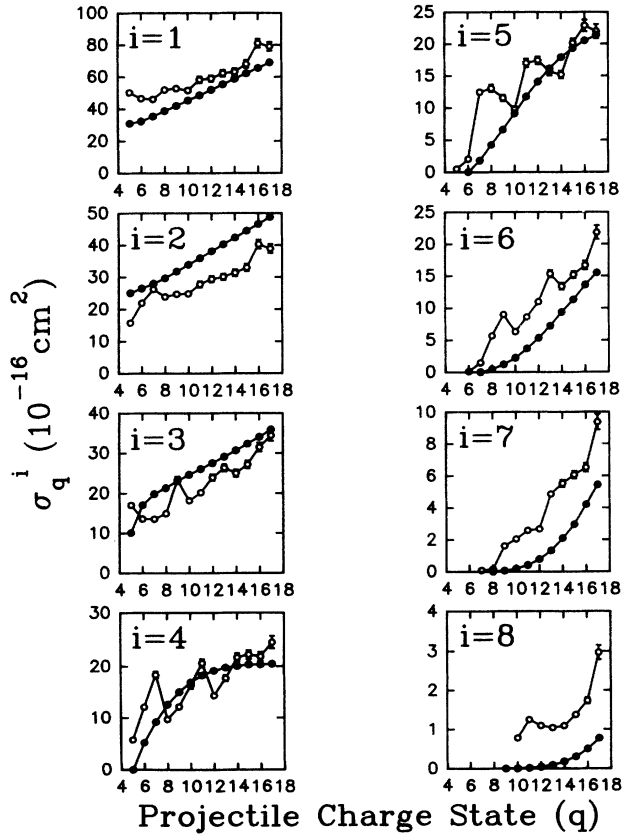

FIG. 5. Experimental (○) and MCBM (●) recoil production cross sections σ_q^i. The MCBM cross sections were obtained by suppressing possible target autoionization and assuming the recoil charge state i to be equal to the number of transferred electrons r.

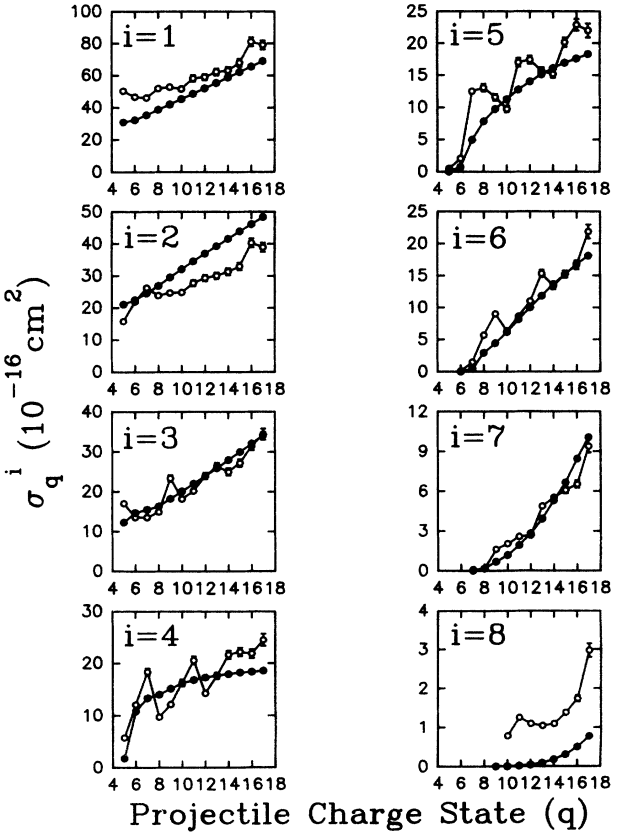

FIG. 6. Experimental (○) and MCBM (●) recoil production cross sections σ_q^i. The MCBM cross sections were obtained by allowing for target autoionization as discussed in text.

of coincidence techniques and the Doppler shift of the projectile Auger lines might help to observe this process. Inner-shell excitation of the target occurs for smaller impact parameters and will be discussed later.

B. Phenomenological and projectile charge-change cross sections (stabilization scheme)

We have shown that the MCBM is capable of accounting for total charge-transfer and recoil production cross sections rather well. The phenomenological cross sections, on the other hand, are somewhat problematic. The transfer of r electrons to the projectile is generally predicted to result in multiply excited states. For $r > 2$, very little is known about such states. Benoit-Cattin *et al.* [20] attempted to disentangle the Auger electron spectra in multielectron transfer collisions of N^{7+} on Ar. They proposed stabilization schemes based on simple arguments such as autoionizing to the nearest continuum limits and minimum electron rearrangement (two-electron transitions) are favored. A major improvement came about with the experiment by Posthumus and Morgenstern [21] where Auger electrons were detected in coincidence with the recoiling ions in Ar^{9+} on Ar collisions. They clearly demonstrated that many of the Auger lines attributed to doubly excited states and associated with the filling of the $2p$ vacancy were in coincidence with recoil charge states $i \geq 3$ suggesting that these states must have been derived from multiply excited projectile states through multiple autoionization processes. Theoretical investigations of multiply excited states are essentially absent except for the calculations of radiative and nonradiative decay rates in triply excited $(3l,3l',nl'')$ N^{4+} by Vaeck and Hansen [33].

In order to account for the phenomenological cross sections a reasonable stabilization scheme is needed. In the absence of even average autoionization and radiative rates and branching ratios for the enormous number of multiply excited configurations of the projectile that are predicted by the MCBM, we propose a stabilization scheme that is based on the cumulative knowledge available from studies of doubly excited states and the few experimental observations concerning multiply excited states. Before outlining the stabilization scheme, we first consider the energy levels of multiply excited states.

We begin with the doubly excited configurations for which good knowledge of the evolution with q of the energy positions of the (4,4) and (5,5) manifolds relative to their nearest continuum levels turned out to be essential. We have used the general purpose relativistic atomic structure program (GRASP[2]) [34] to calculate these energy levels for all incident projectile charge states. In Figs. 7(a)–7(c) we show three examples which illustrate this evolution. We observe that all states belonging to the (4,4) manifold in Ar^{6+**} (core charge $q = 8$) are energetically allowed to autoionize to the $(3,\infty)$ continuum limits, and the same is true for a large fraction of such states in Ar^{12+**} (core charge $q = 14$). However, none of these states are allowed to autoionize to the $(3,\infty)$ continuum limits in Ar^{14+**} (core charge $q = 16$) and therefore the

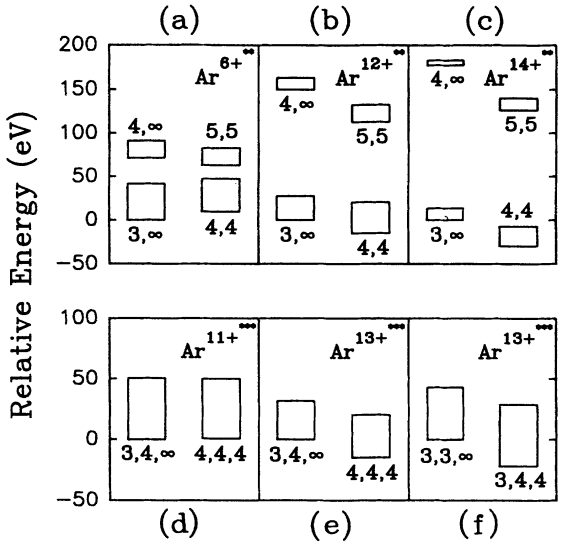

FIG. 7. Energies of doubly and triply excited ionic states relative to the lowest continuum limit shown in each example. The horizontal borders of each box represent the lowest- and highest-energy levels in the corresponding manifold. The evolution with q from energetically allowed to not allowed autoionization of (4,4) states to the $(3,\infty)$ continuum limits [(a)–(c)] and the effect of introducing an additional electron [(d)–(f)] illustrate the need for proper knowledge of the characteristics of the multiply excited states.

only available limits are $(2,\infty)$. A similar trend is observed for the (5,5) manifolds relative to the $(4,\infty)$ limits. This evolution has serious consequences for the stabilization of electrons on the projectile when autoionizing cascades are considered. The behavior is strongly modified for triply excited states as shown in Figs. 7(d)–7(f). For example, for the same core charge $q = 14$ all the (4,4,4) in Ar^{11+**} states are now energetically allowed to autoionize to the $(3,4,\infty)$ limits. Similar evolution is observed for the core $q = 16$ where a large number of the (4,4,4) and (3,4,4) states can autoionize to the $(3,4,\infty)$ and $(3,3,\infty)$ continuum limits. We have investigated this evolution for configurations representing electrons in the same and in different shells of doubly, triply, quadruply and quintuply excited states which were frequently predicted by the MCBM.

With the proper knowledge of the relevant energy levels we propose the following scheme.

(i) The multiply excited states will dominantly stabilize through multiple Auger processes. Radiative stabilization is allowed only if appropriate conditions are realized which will be discussed later.

(ii) Minimum electron rearrangement is dominant in the sense that only two-electron Auger transitions are allowed.

(iii) An Auger transition will proceed to the nearest energetically allowed continuum limit with unit probability; transitions to other continuum limits are assumed to be negligible, as in possible population of nonautoionizing

multiply excited states.

(iv) When many Auger transitions are possible, they proceed according to the following rules. (a) Transitions involving electrons in the same shell proceed first since they generally have higher Auger rates than electrons in different shells. (b) If two or more transitions involving electrons in the same shell are possible, the one involving the more tightly bound electrons will proceed first [e.g., (4,4) will autoionize before (5,5)]. (c) If two or more transitions involving electrons in different shells are possible, the two electrons that spend more time in the vicinity of each other will autoionize first; otherwise the minimum ejected electron energy criterion is imposed and the two electrons giving rise to the lowest-energy continuum electron will autoionize first.

(v) In determining the energy levels and nearest continuum limits associated with a particular Auger transition in a certain configuration, only the electrons participating in the transition in addition to those in equal or lower-lying n's are considered. Higher-lying electrons are neglected. For example, in the configuration (3,4,4,5,6) the two electrons in (4,4) will undergo the first transition and the relevant energy levels and continuum limits are those of (3,4,4), $(3,3,\infty)$, and $(2,3,\infty)$.

(vi) Following each Auger transition a new configuration is realized and all the aforementioned rules are applied once more. If a transition results in the filling of a vacancy in the lowest empty (partially empty) shell, the new energy levels and continuum limits will be those of the initial core charge reduced by one unit.

(vii) If the cascading process results in a final highly asymmetric doubly excited state such as $(3,n_2 \geq 6)$ or $(4,n_2 \geq 8)$, for which the inner electron may stabilize via one or two photon emission processes, radiative stabilization of both electrons is assumed to take place. This situation is encountered when a highly excited electron is denied the opportunity to participate in an Auger process according to the previous rules. At the collision velocity of 0.632 a.u. this electron most likely possesses high angular momentum which reduces the Auger rate in favor of radiative stabilization [35].

Many elements of the scheme (i)–(iii) are consistent with the assumptions and interpretations of Benoit-Cattin *et al.* [20] and Posthumus and Morgenstern [21]. One difference in approach is noted however. We had to restrict ourselves to one decay channel, the most probable one as determined by (iv)–(vii), of any given configuration, while those authors considered different possible decay channels. Taking into account different decay channels would have rendered our attempt to account for the phenomenological cross sections impossible, due to the complete lack of even average branching ratios for the different channels.

Before discussing the results of the phenomenological cross sections some explanatory remarks are made. The collision velocity of 0.632 a.u. results in a likely population of high angular momentum states. We have also shown that the evolution of the energy levels relative to the continuum limits proceeds such that in some cases only a part of the states belonging to a certain manifold may autoionize with the ejection of low-energy electrons. These states are usually the higher states in that manifold which correspond to moderately to high angular momentum states. In such cases, careful assessment of the possibility of an Auger transition with the ejection of a low-energy electron is essential and has been allowed when reasonably probable. Otherwise the transition is taken to proceed to the next group of continuum limits. We show in Fig. 8 three illustrations of stabilization cascades for a core charge $q=16$. We have applied the scheme to about 2400 different configurations predicted by the MCBM where the final recoil and projectile charge states have been determined for each configuration. The corresponding string cross sections have been assigned to the appropriate phenomenological final products. In applying the scheme, the predicted continuous quantum numbers n_t and m_t were quantized by rounding them off to the nearest integers.

The experimental and predicted phenomenological cross sections, in addition to the overlapping experimental results of Liljeby *et al.* [7] and Danared *et al.* [8] obtained at $v \approx 0.1$ a.u., are shown in Figs. 9–12. The predictions reasonably reproduce many of the experimental

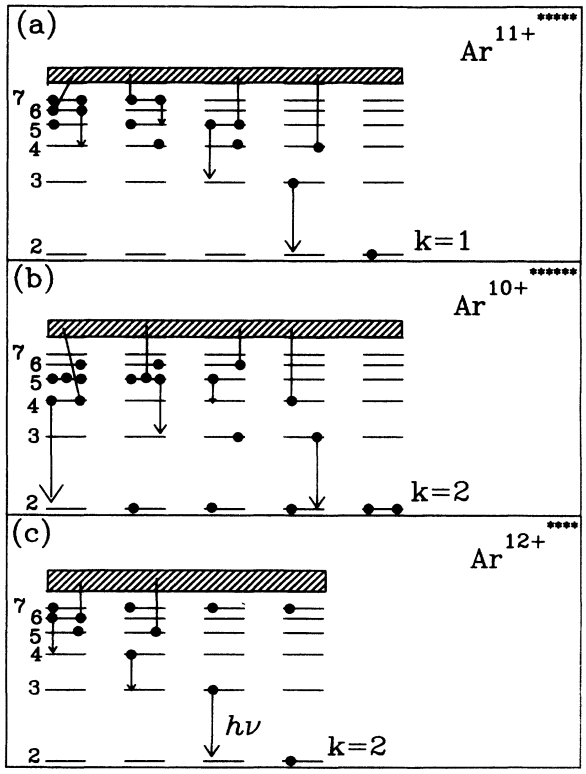

FIG. 8. Three examples of the stabilization of multiply excited ionic states for the core charge $q=16$. The cascades proceed from left to right. (a) The stabilization of one electron through multiple Auger transitions starting with a quintuply excited Ar^{11+}. (b) The stabilization of two electrons through multiple Auger transitions starting with sextuply excited Ar^{10+}. (c) The stabilization of two electrons through multiple Auger transitions and radiative stabilization of the final doubly excited state starting with quadruply excited Ar^{12+}.

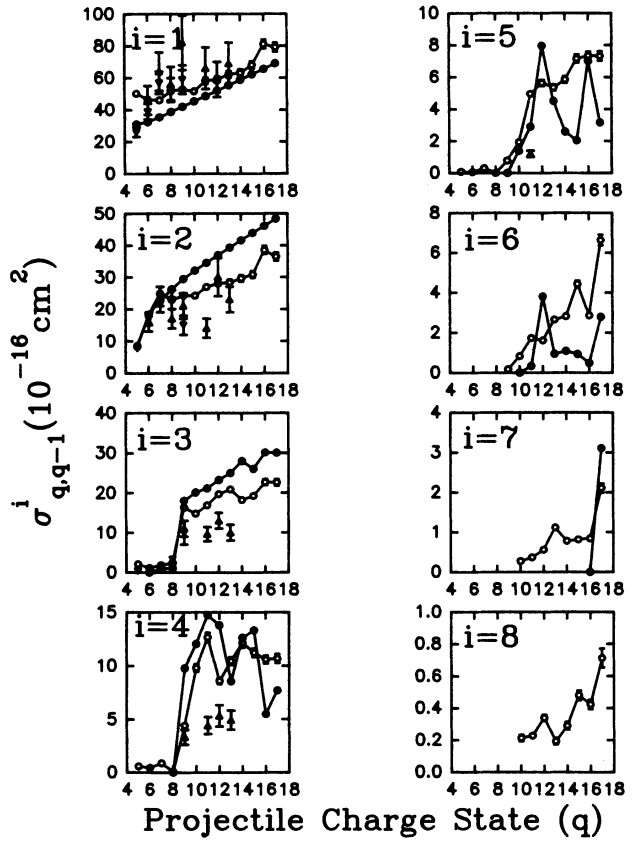

FIG. 9. Experimental (○) and MCBM stabilization (●) phenomenological cross sections $\sigma^i_{q,q-1}$. The data of Liljeby *et al.* [8] (▽) and Danared *et al.* [9] (▲) are also shown.

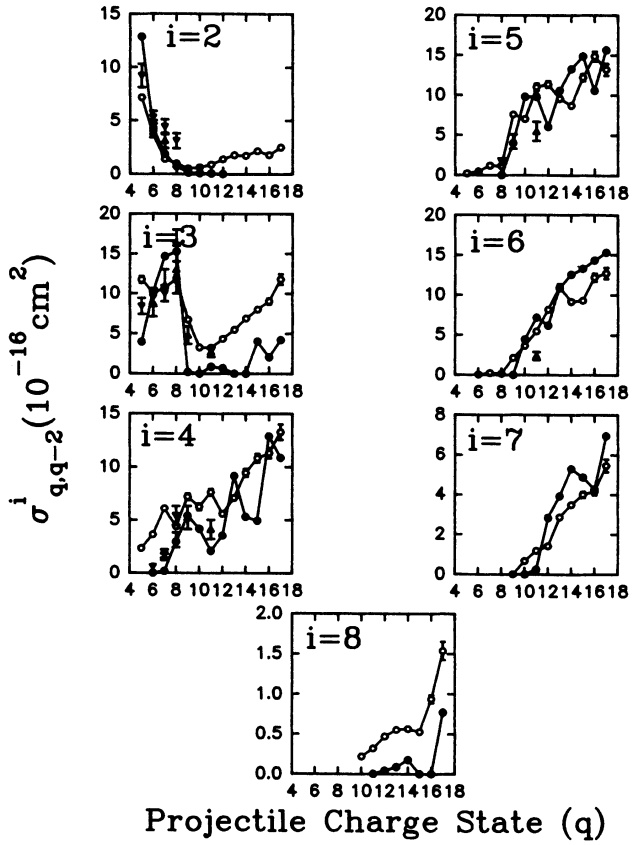

FIG. 10. Experimental (○) and MCBM stabilization (●) phenomenological cross sections $\sigma^i_{q,q-2}$. The data of Liljeby *et al.* [8] (▽) and Danared *et al.* [9] (▲) are also shown.

structures. The quantitative agreement is best for the dominant phenomenological cross sections. Many features are worth noting. For example the sharp increase in $\sigma^3_{q,q-1}$ accompanies the introduction of an L vacancy in the projectile ($q=9$) suggesting that triple-electron capture in this case populates relatively low-lying n's for the L vacancy to participate in the autoionizing stabilization. This is nicely reproduced by the predictions where the dominant population is predicted to be (5,5,5). This cross section, however, exhibits near saturation for $q \geq 12$, although highly excited states [e.g., (7,8,9) for $q=17$] are predicted where two successive Auger transitions are likely to take place. Examination of $\sigma^3_{q,q-2}$ shows a case where enhancement in the stabilization of two electrons is evident with increasing q. This enhancement may result from the population of highly asymmetric triply excited states (n_1,n_2,n_3) where $n_3 \gg n_1,n_2$ through post-collision interactions, such as that proposed by Bachau, Roncin, and Harel [36], which in turn increases the radiative stabilization probability for two electrons. Another possibility is that the first Auger process results in a highly asymmetric doubly excited state such as that described in the stabilization scheme, which then decays radiatively. It is probable that both mechanisms participate. In the calculations, only the latter was taken into account which obviously underestimates the enhancement.

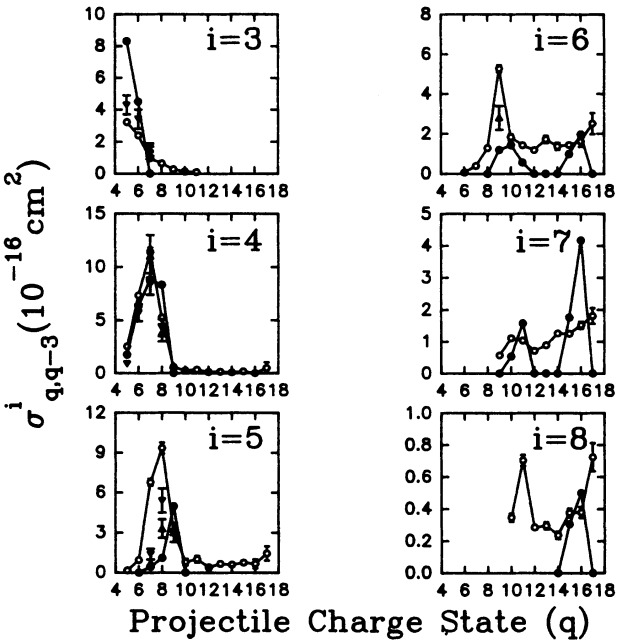

FIG. 11. Experimental (○) and MCBM stabilization (●) phenomenological cross sections $\sigma^i_{q,q-3}$. The data of Liljeby *et al.* [8] (▽) and Danared *et al.* [9] (▲) are also shown.

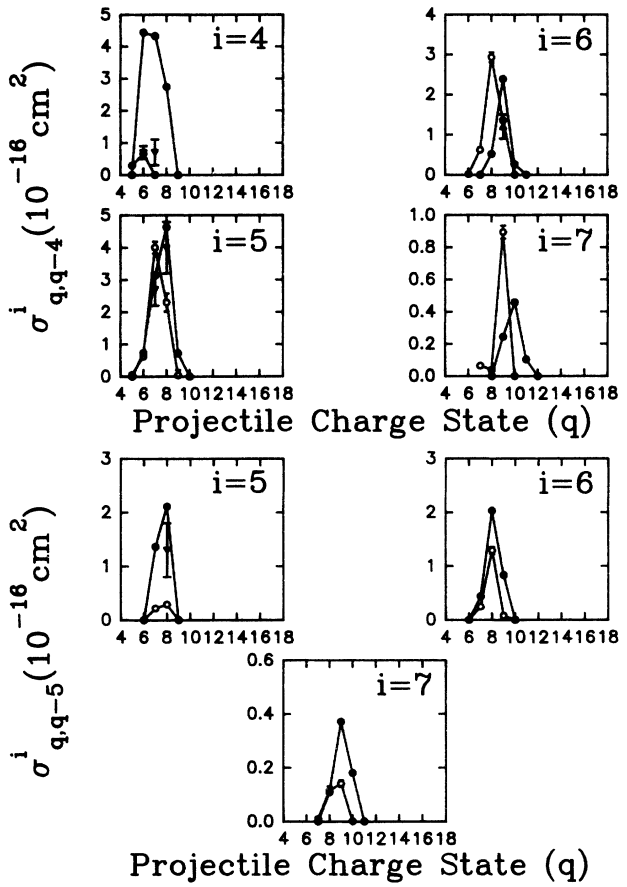

FIG. 12. Experimental (○) and MCBM stabilization (●) phenomenological cross sections $\sigma^i_{q,q-1}$. The data of Liljeby *et al.* [8] (▽) and Danared *et al.* [9] (▲) are also shown.

A similar sharp increase and saturation is observed for $\sigma^4_{q,q-1}$. However, two L vacancies are now observed to participate in the autoionizing stabilization for $q \leq 12$. The saturation may be interpreted through arguments similar to the previous ones noting the obvious enhancement in $\sigma^4_{q,q-2}$. For $i \geq 5$, the cross sections for the stabilization of both one and two electrons are generally increasing with q, but the interpretation of this behavior is more involved since target autoionization seems to play an important role. Nevertheless, the fair success of the MCBM and the stabilization scheme in quantitatively predicting many of these cross sections allow us to make few remarks. The transfer of five or more electrons is not predicted to populate as highly excited levels as those of two or three electrons since they involve tightly bound target electrons. Upon applying the stabilization scheme to such processes, we observed that capturing many tightly bound electrons is no guarantee for retaining two of them. This is a direct result of the previously discussed evolution of the energy levels where $\Delta n_1 = 1$ Auger transitions become energetically allowed in the presence of many neighboring electrons. This increases the number of possible Auger processes and eventually the stabilization of only one electron. On the other hand, configurations with sparsely distributed electrons (loosely and tightly bound) tend to retain two electrons. In the midst of all this there always remains the possibility of radiative stabilization. The stabilization of three or more electrons mostly occurs for $q \leq 10$ where capture of many electrons populates partially filled or low-lying levels. Acceptable agreement with the predictions is obtained for these cases.

We also notice reasonable agreement between our results and those of Liljeby *et al.* and Danared *et al.* for the low recoil charge states in each projectile charge-change channel. Appreciable differences are observed, however, for the higher recoil charge states. While the MCBM predicts the cross sections to be velocity independent for collision velocities less than 1.0 a.u., these differences may suggest otherwise. Further investigations of the velocity dependence of these cross sections and a more extensive data base are needed before definite conclusions can be made.

Model projectile charge-change cross sections were also obtained by summing the phenomenological cross sections over all recoil charge states and are compared to the experiment in Fig. 13. Once more the experimental results are nicely reproduced by the model. It is important, however, to examine the (general) characteristics of the collision systems under study rather than just accounting for the measured cross sections. In Fig. 14(a) we show the experimental average number of electrons lost from the projectile-target system as a function of the incoming projectile and recoil charge states. It is clear that the introduction of L vacancies in the projectiles greatly diminishes the number of retained electrons where on the average two electrons are retained for $i \geq 4$. A dramatic increase in electron loss starts at $q = 9$ but saturates at $q = 10$. While this strongly suggests that two L vacancies are active in L Auger decays for $q = 10$, such a conclusion does not necessarily hold for the higher pro-

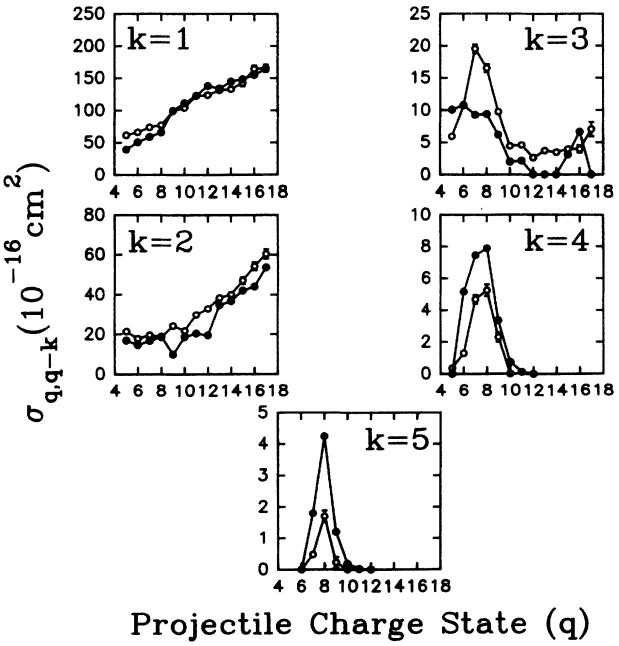

FIG. 13. Experimental (○) and MCBM stabilization (●) projectile charge-change cross sections.

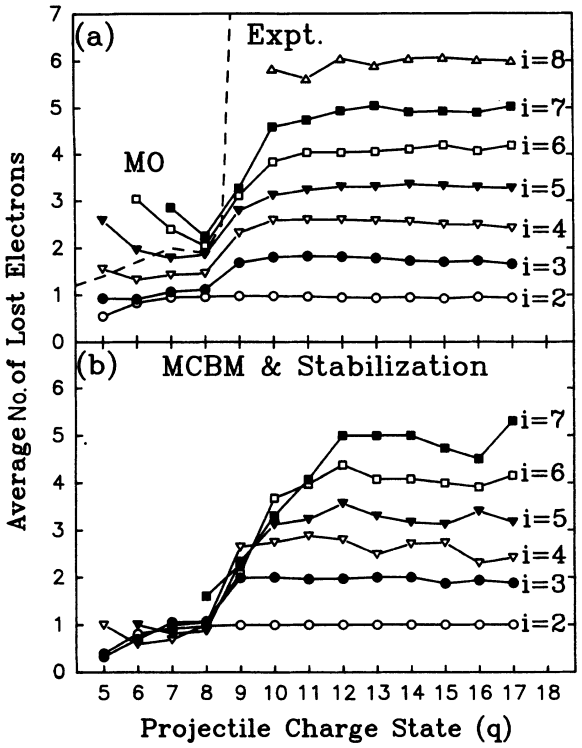

FIG. 14. (a) Experimental and (b) MCBM stabilization average number of electrons lost from the projectile-target collision system. The dashed curve encloses the region (labeled MO) where molecular-orbital promotion mechanism enhances electron loss.

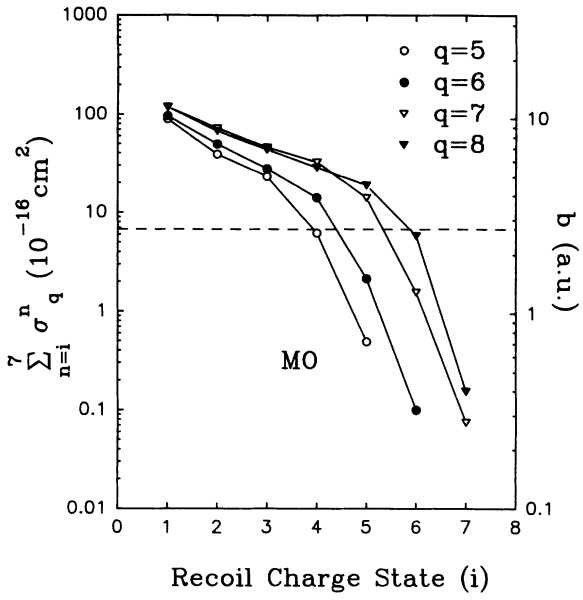

FIG. 15. Sum of recoil production cross sections over recoil charges $\geq i$. The right scale represents the corresponding impact parameters. The regime enclosed by the dashed line (labeled MO) is equivalent to that of Fig. 13(a).

jectile charge states. We found that on the average, to the extent that the stabilization scheme is reliable, the excited configurations result in the ejection of only one L Auger electron with the stabilization of the other electron derived from a singly excited state formed through successive Auger transitions. The predicted average number of lost electrons closely mimics the experimental one as shown in Fig. 14(b) except for $i=8$ and the region labeled MO. It is interesting to note that the presence of a K vacancy in Ar^{17+} makes no appreciable difference. This is consistent with the arguments regarding the radiative stabilization of asymmetric states and the ejection of one L Auger electron.

C. Inner-shell excitation

We have shown in Fig. 14(a) that the electron loss from the projectile-target system is substantially enhanced for $q \geq 9$, which was attributed to the presence of L vacancies and the population of relatively high excited states onto the projectile. We do, however, observe another enhancement in electron loss for projectiles with $q \leq 8$, which is associated with the production of highly charged recoils in the region enclosed by the dashed curve and labeled MO. This cannot be explained on the basis of multielectron capture and the population of autoionizing states since it is predicted to proceed to the partially filled M shell, which is also supported by the experimental points just below the curve. Therefore, another mechanism must be responsible for the additional loss of electrons. Fano and Lichten [37] showed that in hard collisions of Ar^{1+} with Ar, for which the L shells of the collision partners interpenetrate at an internuclear separation less than 0.5 a.u., the creation of one or two L vacancies in the molecule can proceed via the well-known $4f\sigma$ molecular-orbital (MO) promotion mechanism. This promotion will then be followed by electron loss through autoionization. They also indicated that M-shell excitation takes place in the vicinity of $R \sim 1-2$ a.u. To substantiate our claim, we show in Fig. 15 the recoil production cross section for $q \leq 8$ summed in such a way as to represent impact parameters below which recoil charge states greater than i are observed. We have converted the cross section scale to impact parameter scale using $\sigma = \pi b^2$. The region enclosed by the dashed line and labeled MO in Fig. 15 is equivalent to that in Fig. 14. Clearly many of the cross sections give rise to impact parameters in the vicinity of 0.5 a.u., where inner-shell excitation takes place, and others to impact parameters between 1 and 2 a.u. for which M-shell MO excitation is possible. We therefore believe that our earlier inference regarding target excitation in connection with the MCBM predictions was reasonable. A similar connection between inner- and outer-shell processes was noted by Schmidt-Böcking *et al.* [16] and Hermann *et al.* [17]. A direct proof of inner-shell excitation should be possible to obtain through complementary work utilizing Auger electron and photon spectroscopy.

V. CONCLUSION

We have presented measurements of total charge-transfer, recoil production, projectile charge-change, and

phenomenological cross sections for the collision systems 10-keV/u Ar^{q+} ($5 \leq q \leq 17$) on Ar. The measurements verified the predictive powers of the molecular classical overbarrier model. A stabilization scheme utilizing the predictions of the MCBM satisfactorily accounted for the gross phenomenological features. The fair success of the MCBM when target autoionization is assumed to take place and the enhanced electron loss, observed in very hard collisions and attributed to inner-shell excitation, suggest that target outer-shell excitation is an important process. This work clearly demonstrates the need for a more extensive experimental data base of multielectron processes in slow ion-atom collisions and for theoretical investigations of radiative and nonradiative stabilization of multiply excited ionic species.

ACKNOWLEDGMENTS

We would like to thank C. P. Bhalla for helpful suggestions and F. A. Parpia for permitting us to use the GRASP[2] code. This work was supported by the Division of Chemical Sciences, Office of Basic Energy Sciences, Office of Basic Energy Research, U.S. Department of Energy.

[1] M. Barat and P. Roncin, J. Phys. B **25**, 2205 (1992).
[2] H. Klinger, A. Müller, and E. Salzborn, J. Phys. B **8**, 230 (1975).
[3] C. L. Cocke, R. DuBois, T. J. Gray, E. Justiniano, and C. Can, Phys. Rev. Lett. **46**, 1671 (1981).
[4] Edson Justiniano, C. L. Cocke, Tom J. Gray, R. D. DuBois, and C. Can, Phys. Rev. A **24**, 2953 (1981).
[5] E. Justiniano, C. L. Cocke, T. J. Gray, R. DuBois, C. Can, W. Waggoner, R. Schuch, H. Schmidt-Böcking, and H. Ingwersen, Phys. Rev. A **29**, 1088 (1984).
[6] G. Astner, A. Bárány, H. Cederquist, H. Danared, S. Huldt, P. Hvelplund, A. Johnson, H. Knudsen, L. Liljeby, and K.-G. Rensfelt, J. Phys. B **17**, L877 (1984).
[7] L. Liljeby, G. Astner, A. Bárány, H. Cederquist, H. Danared, S. Huldt, P. Hvelplund, A. Johnson, H. Knudsen, and K.-G. Rensfelt, Phys. Scr. **33**, 310 (1986).
[8] H. Danared, H. Andersson, G. Astner, P. Defrance, and S. Rachafi, Phys. Scr. **36**, 756 (1987).
[9] W. Groh, A. Müller, A. S. Schlachter, and E. Salzborn, J. Phys. B **16**, 1997 (1987).
[10] J. Vancura, V. Marchetti, and V. O. Kostroun, in *Proceedings of the VIth International Conference on the Physics of Highly Charged Ions,* edited by P. Richard, M. Stöckli, C. L. Cocke, and C. D. Lin, AIP Conf. Proc. No. 274 (AIP, New York, 1993), p. 113.
[11] P. Hvelplund, A. Bárány, H. Cederquist, and J. O. K. Pedersen, J. Phys. B **20**, 2515 (1987).
[12] H. Anderson, H. Cederquist, G. Astner, P. Hvelplund, and J. O. K. Pedersen, Phys. Scr. **42**, 150 (1990).
[13] P. Roncin, M. N. Gaboriaud, M. Barat, and H. Laurent, Europhys. Lett. **3**, 53 (1987).
[14] R. Ali, V. Frohne, C. L. Cocke, M. Stockli, S. Cheng, and M. L. A. Raphaelian, Phys. Rev. Lett. **69**, 2491 (1992).
[15] M. Sakurai, H. Tawara, I. Yamada, M. Kimura, N. Nakamura, S. Ohtani, A. Danjo, M. Yoshino, and A. Matsumoto, in *Proceedings of the VIth International Conference on the Physics of Highly Charged Ions* (Ref. [10]), p. 101.
[16] H. Schmidt-Böcking, M. H. Prior, R. Dörner, H. Berg, J. O. K. Pedersen, C. L. Cocke, M. Stockli, and A. S. Schlachter, Phys. Rev. A **37**, 4640 (1988).
[17] R. Hermann, M. H. Prior, R. Dörner, H. Schmidt-Böcking, C. M. Lyneis, and U. Wille, Phys. Rev. A **46**, 5631 (1992).
[18] H. Danared, H. Andersson, G. Astner, A. Bárány, P. Defrance, and S. Rachafi, J. Phys. B **20**, L165 (1987).
[19] L. Guillemot, P. Roncin, M. N. Gaboriaud, H. Laurent, and M. Barat, J. Phys. B **23**, 4293 (1990).
[20] P. Benoit-Cattin, A. Brodenave-Montesquieu, M. Boudjema, A. Gleizes, S. Dousson, and D. Hitz, J. Phys. B **21**, 3387 (1988).
[21] J. H. Posthumus and R. Morgenstern, Phys. Rev. Lett. **68**, 1315 (1992).
[22] J. Vancura and V. O. Kostroun, in *Proceedings of the VIth International Conference on the Physics of Highly Charged Ions* (Ref. [10]), p. 120.
[23] S. Martin, A. Denis, J. Désesquelles, and Y. Ouerdane, Phys. Rev. A **42**, 6564 (1990).
[24] S. Martin, A. Denis, Y. Ouerdane, A. Salmoun, A. El Motassadeq, J. Désesquelles, M. Druetta, D. Church, and T. Lamy, Phys. Rev. Lett. **64**, 2633 (1990).
[25] S. Martin, Y. Ouerdane, A. Denis, and M. Carré, Z. Phys. D **21**, s277 (1991).
[26] S. Martin, A. Denis, A. Delon, J. Désesquelles, and Y. Ouerdane, in *Proceedings of the VIth International Conference on the Physics of Highly Charged Ions* (Ref. [10]), p. 206.
[27] H. Ryufuku, K. Sasaki, and T. Watanabe, Phys. Rev. A **21**, 745 (1980).
[28] A. Bárány, G. Astner, H. Cederquist, H. Danared, S. Huldt, P. Hvelplund, A. Johnson, H. Knudsen, L. Liljeby, and K.-G. Rensfelt, Nucl. Instrum. Methods B **9**, 397 (1985).
[29] A. Niehaus, J. Phys. B **19**, 2925 (1986).
[30] H. Cederquist, E. Beebe, C. Biedermann, Å. Engström, H. Gao, R. Hutton, J. C. Levin, L. Liljeby, T. Quinteros, N. Selberg, and P. Sigray, J. Phys. B **25**, L69 (1992).
[31] Martin P. Stockli, R. M. Ali, C. L. Cocke, M. L. A. Raphaelian, P. Richard, and T. N. Tipping. Rev. Sci. Instrum. **63**, 2822 (1992).
[32] W. Steckelmacher, R. Strong, and M. W. Lucas, J. Phys. D **11**, 1553 (1978).
[33] N. Vaeck and J. E. Hansen, J. Phys. B **25**, 3267 (1992).
[34] F. A. Parpia and I. P. Grant, J. Phys. (Paris) Colloq. **4**, C1-33 (1991); F. A. Parpia, I. P. Grant, and C. F. Fischer (unpublished).
[35] R. Ali, C. L. Cocke, M. L. A. Raphaelian, and M. Stockli, J. Phys. B **26**, L177 (1993), and references therein.
[36] H. Bachau, P. Roncin, and C. Harel, J. Phys. B **25**, L109 (1992).
[37] U. Fano and W. Lichten, Phys. Rev. Lett. **14**, 627 (1965).